

Structure and Formation Mechanism of Black TiO₂ Nanoparticles

Mengkun Tian¹, Masoud Mahjouri-Samani², Gyula Eres^{3*}, Ritesh Sachan³, Mina Yoon², Matthew F. Chisholm³, Kai Wang², Alexander A. Puretzky², Christopher M. Rouleau², David B. Geohegan² & Gerd Duscher^{1,3*}

¹Department of Materials Science and Engineering, University of Tennessee, Knoxville, TN 37996, USA

²Center for Nanophase Materials Sciences, Oak Ridge National Laboratory, Oak Ridge, TN 37831, USA

³Materials Science and Technology Division, Oak Ridge National Laboratory, Oak Ridge, TN 37831, USA

* Corresponding authors: E-mail address: eresg@ornl.gov and gduscher@utk.edu

Linear combination and linear least-square fit

Before taking core-loss spectra, the zero-loss peak was confirmed at exact zero eV to ensure the exact positions of peaks in the ELNES. The reference rutile, anatase EELS spectra were taken from Degussa P25, and the reference Ti₂O₃ EELS spectra were taken from Ti₂O₃ purchased from Sigma-Aldrich. These titanium oxides are in NP forms, whose ELNES are very close to the pure ones synthesized by us in oxygen gas (for anatase and rutile) and in He gas (for Ti₂O₃) at a different pressures by PLV. We fit the background with an energy window 400eV-455eV for Ti-L_{2,3} edges and 510-525eV for O-K edges by using a combination of power law and polynomial model $E^{-r} + aE^2 + bE + c$. Here a, b, c and r are fitting parameters, E is the energy. After subtracting the background, intensities of Ti-L_{2,3} edges and O-K edges in the EELS spectra were normalized within energy window 450eV-470eV and 525-550eV, respectively. We then produced linear combinations of EELS spectra of pure TiO₂ and Ti₂O₃ for Ti-L_{2,3} edge part and O-K edge part, respectively, as shown in Figure S1. It should be noted that the energy dispersion of reference spectrum from pure rutile and Ti₂O₃ used in this linear combination is 0.1eV/channel in order to acquire Ti L_{2,3} and O-K edges at the same time. Thus, there is a small reduction of energy resolution (<0.1eV) because of unable to focus zero-loss peak as precise as in the highest energy dispersion (0.025eV/channel) case. We used least-square fitting to find the best fit between the experimental spectra taken at different locations of the rutile particle and the reconstructed spectra yielding the coefficients, as shown in Figure S2. Because the background is subtracted, we estimated the average noise in the pre-ionization edge area. The energy window of fit is 430eV-455eV for Ti-L_{2,3} edge and 510-525 eV for O-K edge. By comparison, the fit difference between experimental spectra and reconstructed spectra is close to the noise level (maximum < 6% for Ti and maximum < 5% for O) at different locations except at 1 nm (~10% for Ti and ~13% for O) where signal-to-noise ratio is relatively low.

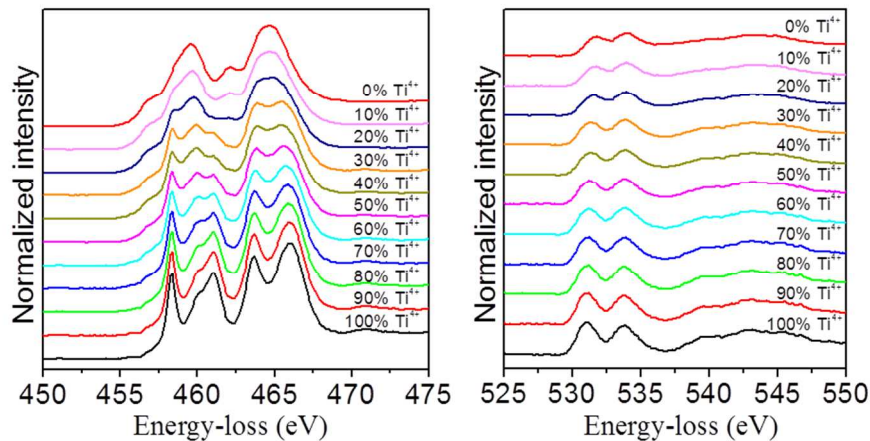


Figure S1. Reconstructed EELS spectra of Ti-L_{2,3} and O-K ELNES from linear combination of pure TiO₂ and Ti₂O₃, respectively. The linear combination of the TiO₂ and Ti₂O₃ shows the transformation of the EELS spectra of Ti-L_{2,3} edge (left) and O-K edge (right) from rutile (100% Ti⁴⁺) to Ti₂O₃.

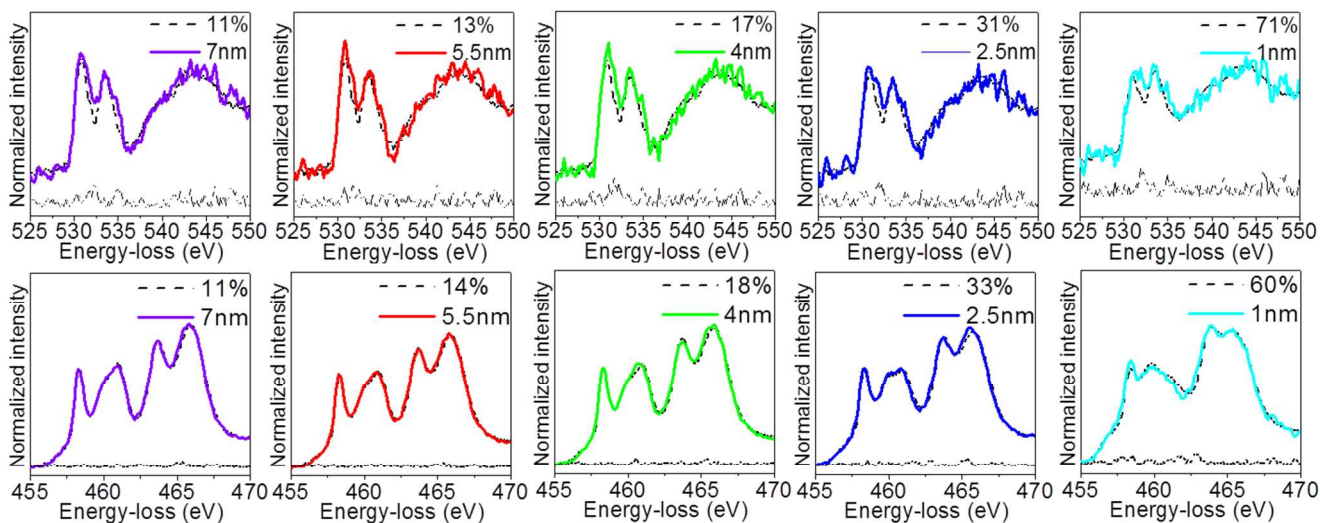


Figure S2. EELS spectra taken at different locations compared to the fits from linear combination from pure rutile and Ti₂O₃. The EELS spectra for both the O-K edge (top) and the Ti-L_{2,3} edge show that rutile features become less pronounced closer to the surface.

Detection geometry effect of EELS spectrum on NPs with different sizes

It should be noted that signal measured at the NP edge is affected by the 1) surface roughness of the NPs, 2) instrument drift during EELS acquisition of roughly one atomic layer and 3) electron-beam broadening. This combination of intrinsic and instrumental factors obscures the identification of Ti₂O₃ at the edge of NPs. The examples ‘S1’ and ‘S2’ in Supplementary Figure S3a represent surface spectra taken at grazing incidence from two different spots of the same rutile NP in Figure 1b. We can clearly observe TiO₂ crystal field splitting features in spectrum ‘S1’, while these features are almost unrecognizable in spectrum ‘S2’, indicating different Ti₂O₃ concentration. However, the significant increased surface-volume ratio in smaller nanoparticles allows to acquire surface spectra with less delocalization.

Figure S3b shows $\sim 100\%$ Ti_2O_3 from fitting the EELS spectrum taken at the surfaces (by summing spectra in order to increase signal-to-noise ratio) of a nanoparticle 4 times smaller the one in Figure S3a. The L_2 - t_{2g} peak of Ti_2O_3 , whose position is quite different with rutile and anatase, unambiguously confirm highest Ti_2O_3 concentration in the surface. However, we didn't perform systematic characterizations on small rutile not only due to the low signal-to-noise ratio, especially for O-K edge, but also concerning the influence of twin boundaries on the ELNES which are rich in the small rutile ($<14\text{nm}$) NPs.

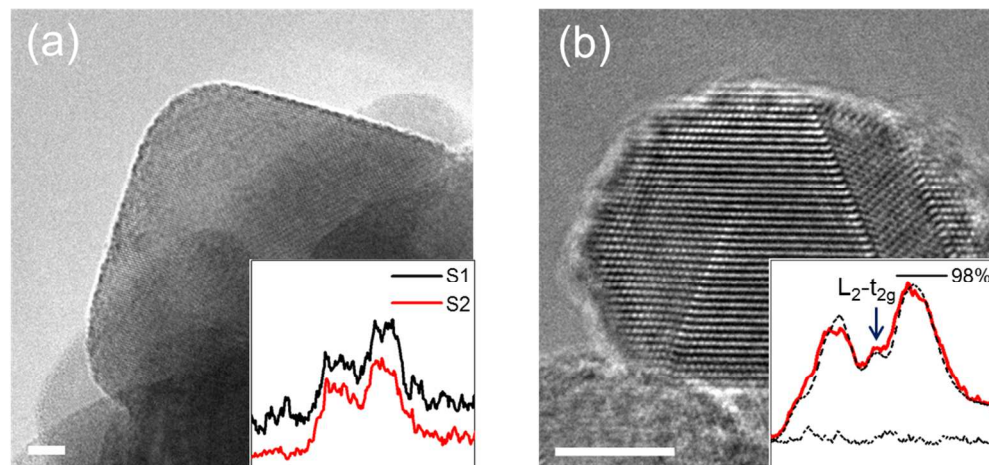


Figure S3. Comparison of EELS spectra taken from the rutile in Figure 1b and a rutile nanoparticle 4 times smaller. (a) HRTEM image of overview of the rutile nanoparticle in Figure 1b. EELS spectra (inset) of surface regions (S1 and S2) acquired at grazing incidence from two different spots, showing different Ti^{4+} concentration. (b) HRTEM image of a rutile nanoparticle viewed in $[111]$ direction. EELS spectrum (inset) was summed from the surfaces, showing Ti_2O_3 characteristic L_2 - t_{2g} peak. The linear least-square fit shows $\sim 100\%$ Ti_2O_3 concentration. Scale bars are 5nm.

Color comparison of nanoparticles synthesized by PLV before and after annealing.

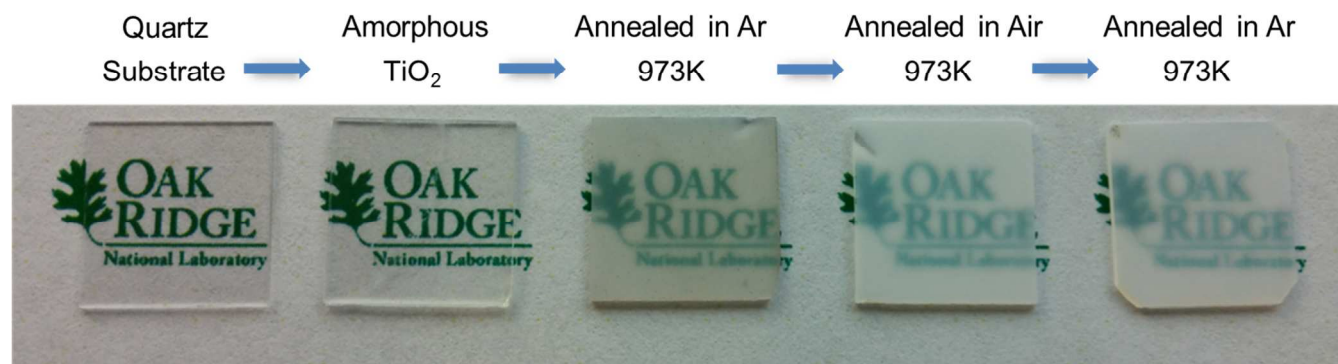


Figure S4. Nanoparticles synthesized by PLV before and after annealing. The color of amorphous TiO_2 nanoparticles is transparent, which turns black after annealing in Ar at 973 K, resulting from formation of Ti_2O_3 shell. This shell can be oxidized by annealing in air, showing white color. This transformation is irreversible as the color of these nanoparticles cannot turn black.

Calculation of rutile/Ti₂O₃ phase transformation by first-principles density functional theory calculation

We performed first-principles density functional theory (DFT) calculations to understand the thermodynamic stabilities of TiO₂ (rutile) and Ti₂O₃ crystals at a given experimental condition. Our total energy calculations adopt the Perdew-Burke-Ernzerh of version of exchange-correlation functional¹ and the projector augmented wave method² for ionic potentials as implemented in the Vienna Ab Initio Simulation Package³. We compare the changes in the Gibbs free energy (G) between TiO₂ and Ti₂O₃, where we assume that extra oxygen atoms upon the structural transformation return to O₂ ideal gas. The free energy changes incorporated with those changes in bulk volumes are negligible for the considered pressure condition. Difference in Gibbs free energies (ΔG) between the two phases can be expressed as:

$$\Delta G(T, P) = U_{TiO_2} + \mu_{TiO_2}(T, P_0) - \frac{1}{2} [U_{Ti_2O_3} + \mu_{Ti_2O_3}(T, P) + \frac{1}{2} (\mu_{O_2}(T, P_0) + U_{O_2} + k_B T \ln(\frac{P}{P_0}))]$$

where we obtained the internal energies U from the DFT calculations and the chemical potentials of each species for a given temperature (T) and oxygen pressure (P) were obtained from experimental data, the NIST-JANAF thermochemical tables⁴. The phase diagram was constructed based on G for a given P and T.

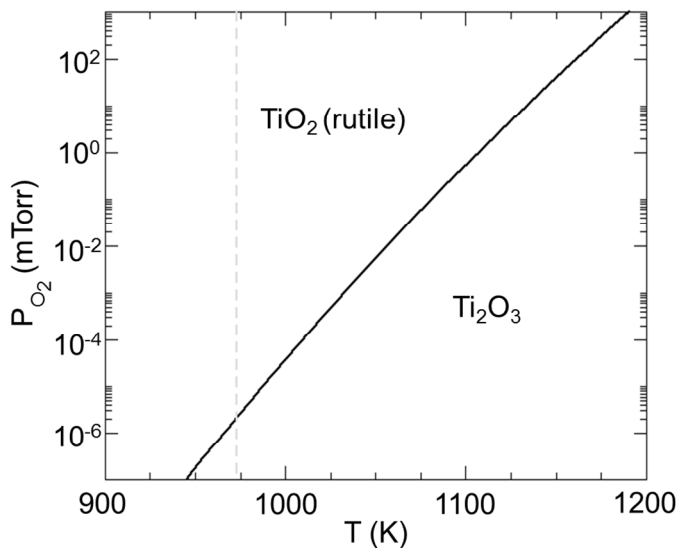


Figure S5. Thermodynamic stabilities of TiO₂ rutile and Ti₂O₃ as a function of the temperature (T) and oxygen pressure (P). The solid line delineates the existence of two phases, and the vertical dashed line guides experimental temperature of 973K.

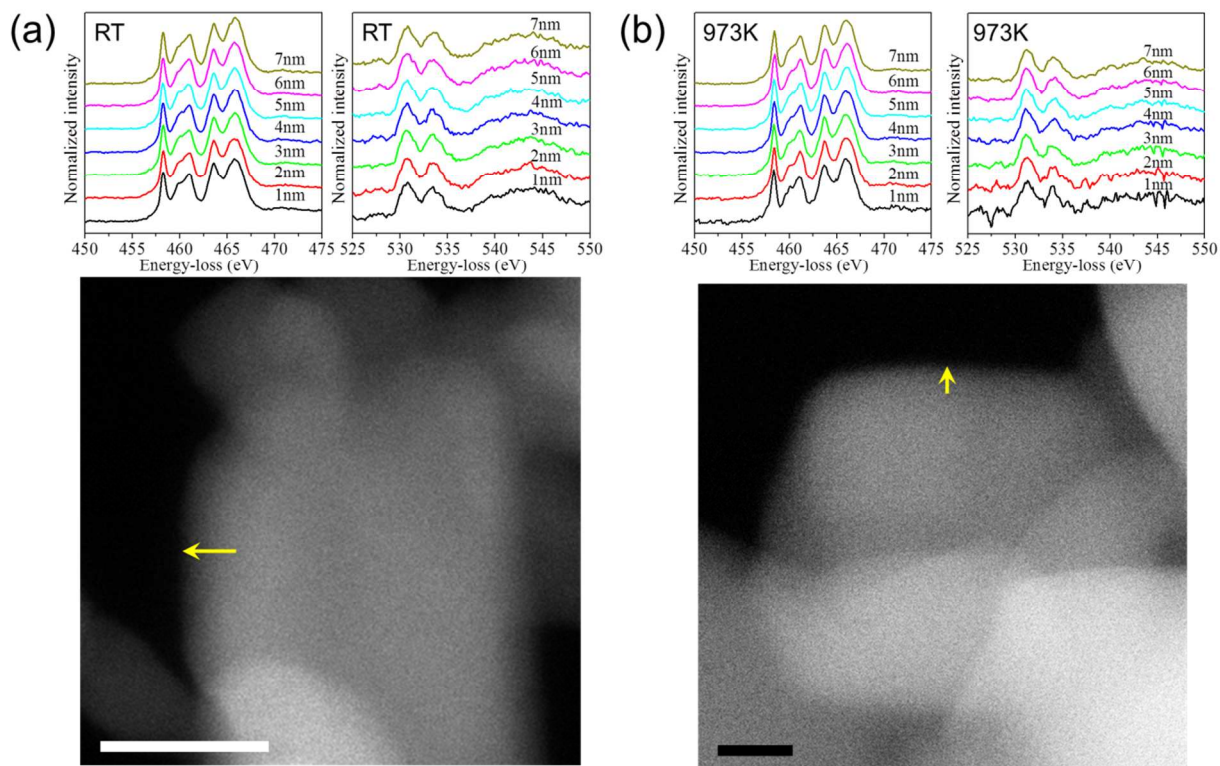


Figure S6. Comparison of EELS spectra taken from crystalline precursor at room temperature (RT) and after annealing. (a,b) EELS spectra taken from Degussa P25 at room temperature (RT)/after annealing in Ar at 973K and the Z-contrast image of the nanoparticles. The yellow arrow indicates the direction where the spectrum image was taken. There is no obvious change in the Ti-L_{2,3} and O-K ELNES of EELS spectra taken from different locations of the crystalline nanoparticles (Degussa P25) before and after annealing. Scale bars are 20nm.

REFERENCE

1. Perdew, J. P.; Burke, K.; Ernzerhof, M. Generalized Gradient Approximation Made Simple. *Phys. Rev. Lett.* **1996**, *77*, 3865-3868.
2. Kresse, G.; Joubert, D. From Ultrasoft Pseudopotentials to the Projector Augmented-Wave Method. *Phys. Rev. B* **1999**, *59*, 1758-1775.
3. Kresse, G.; Furthmuller, J. Efficient Iterative Schemes for Ab Initio Total-Energy Calculations Using a Plane-Wave Basis Set. *Phys. Rev. B* **1996**, *54*, 11169-11186.
4. <http://Kinetics.Nist.Gov/Janaf/>. (August 20th, 2015)